

ORIGINAL ARTICLE

X-chromosome linked inhibitor of apoptosis protein inhibits muscle proteolysis in insulin-deficient mice

XH Wang¹, J Hu¹, J Du² and JD Klein¹

¹Renal Division, Department of Medicine, Emory University, Atlanta, GA, USA and ²Nephrology Division, Baylor College of Medicine, Houston, TX, USA

Loss of muscle protein is a serious complication of catabolic diseases and contributes substantially to patients' morbidity and mortality. This muscle loss is mediated largely by the activation of the ubiquitin–proteasome system; however, caspase-3 catalyzes an initial step in this process by cleaving actomyosin into small protein fragments that are rapidly degraded by the proteasome-dependent proteolytic pathway. We hypothesized that X-chromosome linked inhibitor of apoptosis protein (XIAP), an endogenous caspase-3 inhibitor, would block this first step in the cleavage of actomyosin that would make XIAP a candidate for treating muscle wasting. To determine if XIAP could attenuate muscle protein degradation, we used a recombinant lentivirus (Len-XIAP)

encoding the full-length human XIAP cDNA to express XIAP in vivo. In muscle of streptozotocin-treated insulin-deficient mice, total muscle protein degradation, caspase-3 activity, and myofibril destruction were increased while XIAP was decreased. Overexpression of XIAP in these mice attenuated the excessive muscle protein degradation. Increased proteasome activity, caspase-3 activity and myofibril protein breakdown were all reduced. The ability of XIAP to prevent the loss of muscle protein suggests that XIAP could be a therapeutic reagent for muscle atrophy in catabolic diseases.

Gene Therapy (2007) 14, 711–720. doi:10.1038/sj.gt.3302927; published online 22 February 2007

Keywords: muscle protein degradation; XIAP; diabetes mellitus; lentivirus; gene transfer; caspase-3

Introduction

Loss of lean body mass in catabolic states is associated with increased morbidity and mortality.^{1,2} The loss of muscle protein owing to disease, inactivity,³ and aging^{4,5} is a widespread phenomenon known as muscle wasting or atrophy, which occurs in clinical conditions characterized by insulin deficiency and/or insulin resistance including diabetes mellitus,^{6,7} chronic renal failure,⁸ trauma,⁹ burn injury¹⁰ and heart failure.^{11,12} Regardless of the underlying cause, there are common mechanisms that are part of the muscle wasting process in many catabolic conditions.

One important mechanism of muscle wasting involves activation of the ubiquitin–proteasome proteolytic system. This system is activated by a variety of physiological stimuli including insulin deficiency.¹³ We find that accelerated muscle protein degradation in streptozotocin (STZ)-induced insulin-deficient animals is because of activation of the ubiquitin–proteasome system;^{13,14} however, this system cannot directly degrade myofibrillar proteins.¹⁵ These proteins must first be cleaved by caspase-3 into constituent protein fragments to be degraded by the proteasome-dependent proteolysis

system. The appearance of a 14-kDa actin fragment is a biomarker of myofibrillar protein breakdown.¹⁶

The rate of protein degradation is regulated not only by the presence of proteolytic enzymes, but also by the presence of endogenous protease inhibitors. Inhibitor of apoptosis proteins (IAPs) are endogenous inhibitors of caspase activity and should block caspase-3-induced muscle protein degradation when overexpressed in skeletal muscle cells. To date, seven members of the IAP protein family have been identified in humans¹⁷ and are the only known endogenous inhibitors of caspases.¹⁸ IAPs function by binding to and directly inhibiting caspases-3, -7 and -9.^{19,20} X-chromosome linked inhibitor of apoptosis protein (XIAP) is the most potent member of the IAP family. XIAP inhibits the caspases that participate in the initiation of the apoptosis cascade (e.g. caspase-9) as well as those that participate in terminal events of the apoptosis cascade (e.g. caspase-3).¹⁸ Extensive data from both *in vitro* and *in vivo* systems have demonstrated that increasing XIAP can suppress apoptosis triggered by diverse stimuli such as growth factor withdrawal, staurosporine and tumor necrosis factor α (TNF α).^{21–23} On the basis of these findings, we hypothesized that overexpressing XIAP in skeletal muscle would block caspase-3 activity and decrease diabetes-induced muscle atrophy. To test this hypothesis, we used an acute diabetic mouse model. We found that the amount of XIAP was decreased when the proteolytic systems were stimulated by STZ in the insulin-deficient mice. To determine whether XIAP could attenuate the excessive muscle protein degradation induced by insulin

Correspondence: Dr XH Wang, Renal Division, Emory University, School of Medicine, M/S 1930/001/1AG, 1639 Pierce Dr, WMB 338, Atlanta, GA 30322, USA.

E-mail: xwang03@emory.edu

Received 12 September 2006; revised 21 December 2006; accepted 8 January 2007; published online 22 February 2007

deficiency, we introduced a recombinant lentivirus expressing the coding region of human XIAP into the skeletal muscle of mice by intra-muscular injection. Increasing XIAP through lentivirus transduction reduced muscle protein breakdown by blocking caspase-3 activation and attenuated the proteasome-dependent proteolytic pathway.

Results

Protein degradation, caspase activity and XIAP levels in insulin-deficient mice

To examine muscle protein catabolism in intact animals, we induced insulin deficiency in 6-week-old mice by STZ injection and compared them to pair-fed, vehicle-injected mice. After 7 days, we measured protein degradation in soleus (predominately oxidative, red fibers) and plantaris (predominately glycolytic, white fibers) muscles of these mice. The rate of total protein degradation in the soleus muscle of insulin-deficient mice was 65.1% higher than the rate measured in soleus muscles of control mice. Protein degradation in plantaris muscles of insulin-deficient mice was 49.5% higher than that in muscle of control mice (Figure 1a, $P < 0.05$). The rate of protein

degradation was still high when either soleus or plantaris muscle was incubated with protease inhibitors to block both lysosomal and calcium-dependent proteolytic pathways (Figure 1a). However, MG132, a proteasome inhibitor, blocked the increase in protein degradation induced by insulin deficiency (Figure 1b). These data indicate that the accelerated muscle protein degradation in insulin-deficient mice is owing to activation of a proteasome-dependent proteolytic system.

Caspase-3 can be activated by either caspase-8 or -9.²⁴ We measured caspase-3, -8 and -9 activities in hind-limb muscle lysates of control and STZ-treated mice. There was no significant change in caspase-8 between control and STZ-treated mice (data not shown). The activity of caspase-3 and -9 was significantly higher in the skeletal muscle of insulin-deficient mice when compared with pair-fed control mice (Figure 2a, $P < 0.05$). Consistent with an increase in caspase activities, the amount of the anti-apoptotic protein XIAP was significantly decreased in skeletal muscle of insulin-deficient mice vs pair-fed control mice (Figure 2b, $P < 0.01$). To determine if the activation of the caspases would lead to actomyosin degradation, myofibrillar lysates were prepared by subjecting the muscle to hypotonic shock and then lysates were assessed for actin proteins by immunoblot-

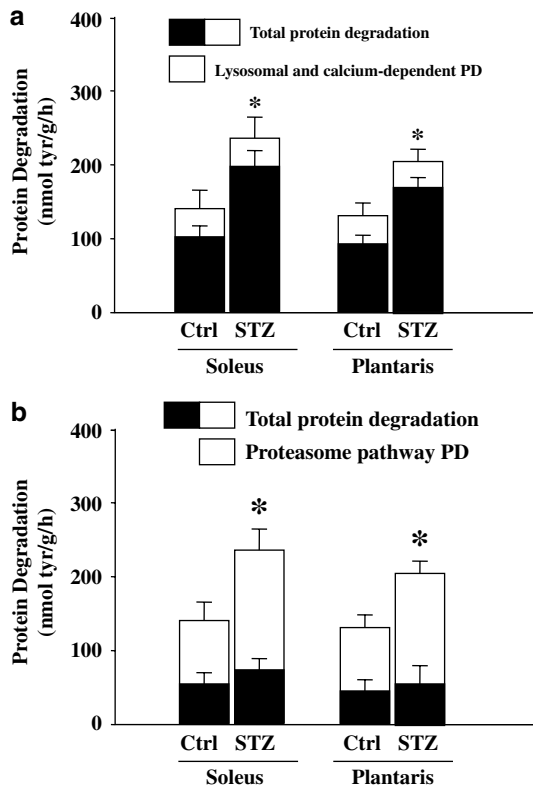


Figure 1 Protein degradation in skeletal muscle of STZ-induced insulin-deficient mice. These bar graphs show (a) rates of total protein degradation (open bar plus solid bar) and lysosomal and calcium-dependent protease pathways (open bar) in soleus and plantaris muscles from control (ctrl) and diabetic (STZ) mice. Data: mean \pm s.e., $n = 6$, $*P < 0.05$, (b) rates of total protein degradation (open bar plus solid bar) and the proteasome proteolytic pathway (open bars) in the soleus and plantaris muscle from control (ctrl) and diabetic (STZ) mice. Degradation by the proteasome-dependent proteolysis was measured using MG132, a proteasome inhibitor. Data: mean \pm s.e., $n = 6$, $*P < 0.05$.

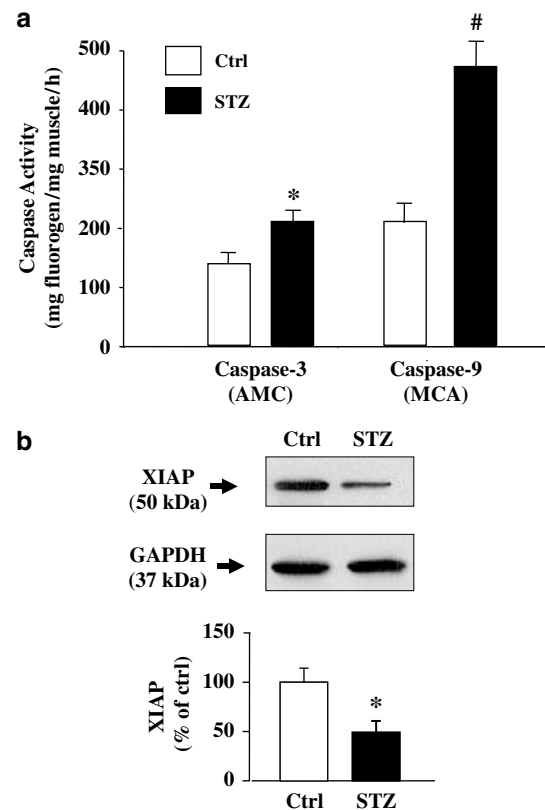


Figure 2 The changes of caspase and XIAP in STZ-induced insulin-deficient mice. (a) Fluorogenic substrates were used to assess caspase activities (Ac-DEVD-AMC for caspase-3 and Ac-LEHD-MCA for caspase-9) in gastrocnemius muscle of STZ and control (ctrl) mice. The bars show the difference between the substrate cleavage in the presence and absence of caspase-3 or -9 inhibitors. (b) Western blot of XIAP in gastrocnemius muscle of STZ and control (ctrl) mice. XIAP densities were normalized to the GAPDH loading controls and are presented as % of control density. Data: mean \pm s.e., $n = 6$ pairs, $*P < 0.01$, $\#P < 0.001$.

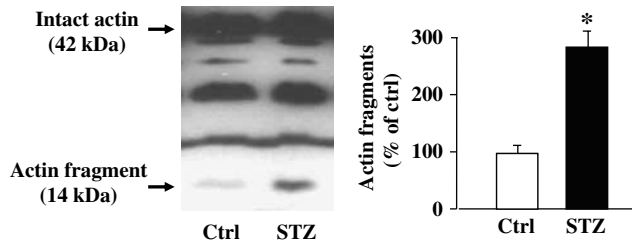


Figure 3 Myofibril protein cleavage in skeletal muscle of STZ-induced insulin-deficient mice. Western blot of gastrocnemius showing the 14 kDa actin fragment resulting from the activation of myofibril protein breakdown. The bar graph shows that the quantity of actin fragments calculated by the density of 14 kDa bands divided by the density of 42 kDa actin bands as a percent of control values. Insulin-deficient mice (black bars) had substantially higher levels of the actin fragment compared to control mice in skeletal muscle (data: mean \pm s.e., $n = 6$, * $P < 0.001$).

ting. A major band corresponding to the expected size of monomeric skeletal muscle actin (42 kDa) was present, but a second, 14 kDa actin fragment indicative of caspase-3 cleavage, was also present and was increased with insulin deficiency (Figure 3, $P < 0.001$). Therefore, insulin-deficient mice exhibit increased protein degradation, increased caspase activity and decreased XIAP levels.

Transduction efficiency of Lentivirus in muscle tissue

To investigate if increased XIAP attenuated proteolytic responses in muscle, we first tested the transduction efficiency of lentivirus-mediated gene transfer in skeletal muscle using Len-enhanced green fluorescence protein (EGFP), a recombinant lentivirus that encodes the EGFP gene. A three-plasmid expression system was used to generate lentivirus particles: a packaging plasmid, an envelope plasmid and an expression vector. The packaging plasmid cytomegalovirus (pCMV Δ R8.91) contained the human CMV (hCMV) immediate early promoter to drive the expression of the transduced gene (EGFP, XIAP, etc.). This plasmid was designed to be defective for the production of any viral accessory proteins. Lentiviruses that have been pseudotyped with surface glycoproteins from different envelope plasmids allow preferential transduction of specific cell types.²⁵ We produced EGFP lentiviruses by co-transfecting HEK293 cells with the expression vector (pCCL.EGFP), the packaging plasmid (pCMV Δ R8.91) and one of five different envelope plasmids (Figure 4A) as follows: (a) VSV-G, *Rhabdoviridae* vesicular stomatitis virus G; (b) Mokola, mokola virus; (c) EbolaZ, Filovirus Ebola Zaire virus; (d) LCMV, arenavirus lymphocytic choriomeningitis virus; and (e) murine leukemia virus (MuLV), oncovirus MuLV. We used these to screen for the optimal conditions for muscle transduction. Each of the five Len-EGFPs (same titer (10^7 transduction units (TU)), freshly prepared viruses) was slowly injected into the back of hind-limb muscles of newborn mice. Mice were killed 30 days after the injection. Gastrocnemius muscles were harvested and EGFP content determined. We compared the percentage of positive fibers in the gastrocnemius muscles. MuLV-enveloped Len-EGFP had the highest transduction efficiency (50–60%) in muscle fibers (Figure 4B, $P < 0.05$ vs other four envelope plasmids). However, using only one injection, the animal-to-animal variability was large.

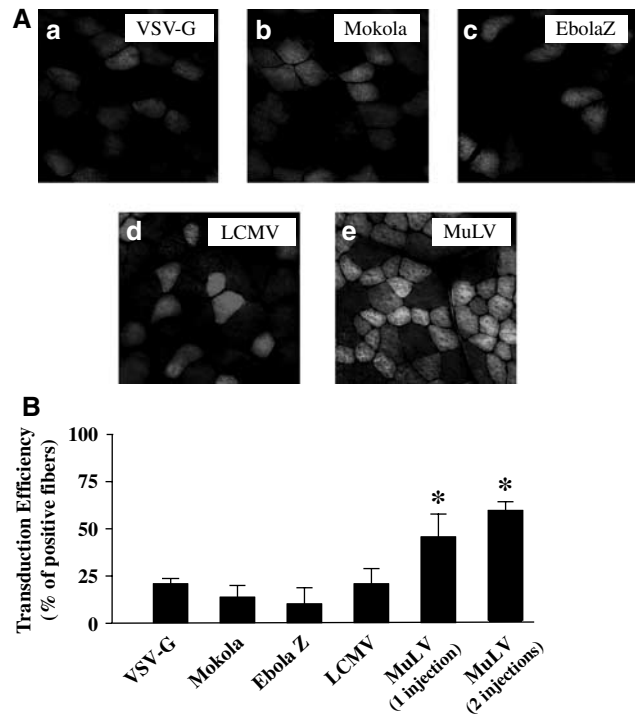


Figure 4 Transduction efficiency of lentiviruses. (A) Shown are cryosections of gastrocnemius muscle transduced with equal volumes of concentrated Len-EGFP (10^7 TU) pseudotyped with different envelope glycoproteins. Envelope plasmids were derived from the following viruses: (a) VSV-G, *Rhabdoviridae* vesicular stomatitis virus G; (b) Mokola, mokola virus; (c) EbolaZ, Filovirus Ebola Zaire virus; (d) LCMV, arenavirus lymphocytic choriomeningitis virus; (e) MuLV, oncovirus MuLV. Muscles were collected 30 days after injection of the newborns (Materials and methods). Identical settings (microscope, magnification ($\times 200$), exposure, camera settings) were used for all muscles compared. (B) Bars show the transduction efficiency as a percentage of positive cells for the sections. In one group of mice, Len-EGFP pseudotyped with MuLV envelope plasmid was boosted with a second injection at 14 days. Data: mean \pm s.e., $n = 5$, * $P < 0.05$.

We compared the single-injection technique with a multiple-injection protocol, where the second injection was administered in the same place after 14 days and third injection was given at 28 days after the first injection. We found that two injections produced better transduction efficiency than a single (54 ± 13 vs $61 \pm 5\%$) injection, whereas three injections did not further increase the transfection efficiency ($62 \pm 4\%$). We chose two injections as our standard protocol to maximize our transduction efficiency and minimize animal-to-animal variability.

To investigate whether an increase in XIAP would attenuate proteolytic responses in muscle, Len-XIAP (10^8 TU in Hank's solution) or virus without an exogenous gene (Len-control (Len-ctrl)) was transduced in the muscle of newborn mice. Mice were killed 4 weeks after the second injection. Individual muscles were dissected and the amount of XIAP in the muscle lysates was determined by Western blot. XIAP expression was sharply increased in gastrocnemius, soleus and plantaris muscle, but not in extensor digitorum longus (EDL) muscle compared with Len-ctrl-injected muscles (Figure 5). The transduction efficiency appeared to be related to the position of the muscles relative to the

injection site, that is, greater transduction efficiency was observed proximal (gastrocnemius) to the injection site than distal (EDL).

Effect of XIAP on protein degradation in insulin-deficient mouse muscle

To determine the effect of XIAP on lean body mass, we measured physiological parameters of the virus-injected mice (Table 1), including the body weights and individual muscle weights at 7 days after STZ treatment. The body weights of Len-XIAP mice (groups 3 and 4) were similar to Len-ctrl mice (groups 1 and 2) before STZ injection. Body weights of STZ mice (group 2) were decreased by 12% compared to the control mice (group 1), but in the XIAP mice, STZ (group 4) caused only a 6% drop in body weight compared to the XIAP-treated control mice (group 3). In both sets of mice (with or without XIAP transduction in muscle) STZ-treated diabetic mice had significantly higher blood sugar (300 STZ vs 130 mg/dl control) and 43% decreased plasma insulin levels when compared with pair-fed controls ($P < 0.01$). The soleus, plantaris and EDL muscles of insulin-deficient mice (group 2) weighed significantly less than the muscles of control mice (group 1) (19, 16.5 and 22%, respectively; $P < 0.05$). Within the XIAP-treatment groups, the STZ-treated mice (group 4) showed a tendency for the soleus and plantaris muscles to be smaller relative to the XIAP control mice (group 3) (7 and 5%, respectively), but the differences did not reach statistical significance (group 3 compared with group 4). The muscles of the diabetic XIAP-treated mice (group 4) were, however, significantly larger than the non-XIAP-treated diabetic mice (group 2), suggesting that the XIAP

protected the diabetic mice from muscle loss. The EDL muscles from the XIAP mice, which showed very low XIAP content (Figure 3c), did not show the same protection.

The rate of protein degradation was measured as the release of free tyrosine in the isolated soleus and plantaris muscles in the presence of cycloheximide to inhibit tyrosine reutilization. As muscle neither synthesizes nor degrades tyrosine, its accumulation reflects the rate of total protein degradation. Insulin deficiency increased protein degradation. Increasing the amount of XIAP by Len-XIAP transduction resulted in a marked decrease in the insulin deficiency-induced protein degradation (Figure 6a) in both soleus and plantaris muscles. Having determined that accelerated muscle protein degradation was because of activation of the proteasome-dependent proteolytic pathway in non-transduced insulin-deficient mice (Figure 1b), we asked which protein degradation pathway was blocked by XIAP. We incubated one plantaris muscle under basal conditions and the contra-lateral muscle with MG132 to inhibit proteasome function. XIAP blocked the increase in total proteolysis by blocking the proteasome dependent proteolysis induced by STZ (Figure 6b). The same pattern was observed in soleus muscle (data not shown). To explore further whether the increase in muscle proteolysis in the insulin-deficient mice was related to activation of the proteasome system, we isolated the proteasome from hind-limb muscles from four different groups of mice and measured their activity. The 26S proteasome chymotryptic-like peptidase activity was increased 1.9-fold in the muscle of insulin-deficient mice. The 20S proteasome activity was also significantly increased 1.4-fold. Increasing the amount of XIAP significantly suppressed this increased enzyme activity in both 26S and 20S proteasome (Figure 7).

Muscle fiber cross-sectional area is a good measure of muscle atrophy and hypertrophy because it avoids the confounding effects of extracellular volume.²⁶ Cross-sectional area was determined in frozen sections of plantaris muscles using an anti-laminin antibody to detect the muscle membranes. For each muscle cross-section (Figure 8a), 500 muscle fibers were examined. Muscle fiber size from STZ-treated mice ($847.7 \mu\text{m}^2 \pm 128.7$) was significantly smaller than STZ-treated XIAP mice ($998.7 \mu\text{m}^2 \pm 145.42$; $P < 0.05$). Fiber area frequency distribution revealed a clear increase in the percentage of small fibers (a leftward shift) in STZ-treated mice (Figure 8b). XIAP overexpression in STZ-treated mice suppressed the leftward shift in the fiber size distribution.

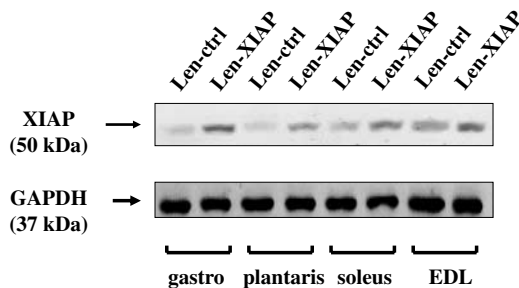


Figure 5 Overexpression of XIAP in skeletal muscle of mice. The Western blot shows increased XIAP in muscles transduced with Len-XIAP vs Len-ctrl: gastrocnemius (gastro), soleus, plantaris and EDL. GAPDH is provided as a loading control.

Table 1 Physiologic parameters

Group			Body Weight (g)		Blood sugar (mg/dl)	Plasma insulin (mg/ml)	Muscle mass (mg)		
			Before	After			Soleus	Plantaris	EDL
1	Len-Ctrl	Ctrl	17.3 ± 0.6	17.8 ± 0.8	130 ± 5	1.14 ± 0.11	6.3 ± 0.2	8.5 ± 0.8	7.6 ± 0.1
2		STZ	17.4 ± 0.3	15.3 ± 0.7*	310 ± 51*	0.65 ± 0.12*	5.1 ± 0.3*	7.1 ± 0.9*	5.9 ± 0.1*
3	Len-XIAP	Ctrl	17.8 ± 0.3	18.4 ± 0.5	131 ± 6	1.16 ± 0.21	6.9 ± 0.2	8.6 ± 0.8	7.8 ± 0.4
4		STZ	17.6 ± 0.4	16.5 ± 0.6*	295 ± 45*	0.75 ± 0.13*	6.4 ± 0.2 [#]	8.1 ± 0.9 [#]	6.9 ± 0.4*

Abbreviations: Ctrl, control, EDL, extensor digitorum longus; STZ, streptozotocin; XIAP, X-chromosome linked inhibitor of apoptosis protein. All data present as mean ± s.e.; n = 6/group; * $P < 0.05$ vs group 1; [#] $P < 0.05$ vs group 2.

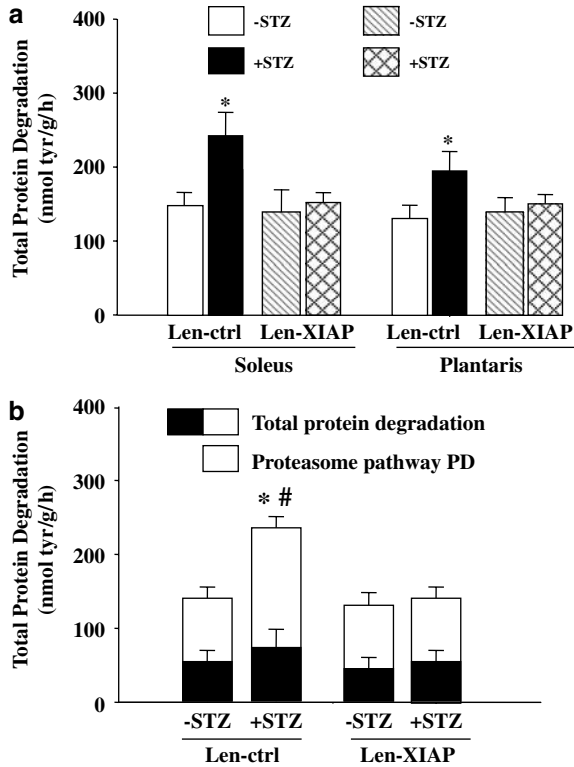


Figure 6 Effect of XIAP on protein degradation in insulin-deficient mice. Mice were transduced with Len-XIAP, then after 6 weeks mice were made insulin deficient by STZ injection. (a) Soleus and plantaris muscle was harvested, and total protein degradation was measured by tyrosine release assay. (b) MG132 was added to the incubation buffer for one muscle from each animal. This bar graph provides rates of total protein degradation (open bar plus solid bar) and the proteasome proteolytic pathway (open bars) from the plantaris muscle of control (ctrl) and diabetic (STZ) mice. Data: mean \pm s.e., $n = 6$, * $P < 0.05$ for total proteolysis Len-ctrl +STZ vs Len-ctrl - STZ and Len-XIAP +STZ, # $P < 0.05$ for proteasome-dependent proteolysis of Len-ctrl +STZ vs Len-XIAP +STZ, $n = 6$.

Effect of XIAP on myofibrillar protein cleavage and caspase activation

To prove that XIAP could block excessive protein degradation by inhibiting caspase-3, we measured the caspase-3 activity in muscle after transduction with Len-XIAP or Len-ctrl. The activity of caspase-3 was significantly higher in the skeletal muscle of insulin-deficient mice vs pair-fed control mice (Figure 9, $P < 0.05$). The activation of caspase-3 induced by insulin deficiency was blocked by increasing XIAP. Higher XIAP also attenuated caspase-9 activity. Caspase-3 activation in muscle leaves a characteristic 14 kDa actin fragment as a 'footprint' for myofibrillar protein degradation. The amount of actin fragment was 2.8-fold higher in the gastrocnemius muscle of STZ-treated insulin-deficient mice when compared to controls. However, in the Len-XIAP-transduced mice, in the presence of the insulin deficiency, the actin fragment was significantly decreased compared with STZ-treated control mice (Figure 10, $P < 0.05$), indicating that XIAP blocked the actin protein breakdown. Both myofibrillar protein cleavage and caspase activation were blocked by increasing the amount of XIAP in muscles of insulin-deficient mice.

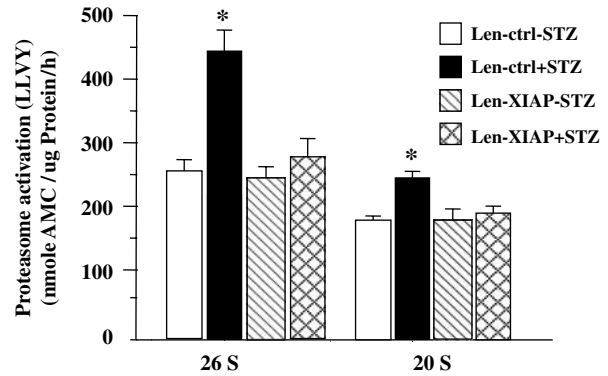


Figure 7 Effect of XIAP on proteasome activation in insulin-deficient mice. Proteasome activity was measured using a fluorogenic substrate LLVY-AMC, with or without the proteasome inhibitor lactacystin (200 μ M). The difference between activity levels in the presence and absence of inhibitor was used to calculate proteasome activity. The bars represent AMC released during a 2-h incubation. Data: mean \pm s.e., $n = 4$, * $P < 0.05$ vs Len-ctrl -STZ and Len-XIAP+STZ.

Discussion

Our report provides evidence that XIAP, an anti-apoptosis protein, is decreased in the muscle of insulin-deficient mice. An increase in XIAP results in resistance to total protein loss (Figure 6a) and myofibrillar protein breakdown (Figure 10) in the muscles of STZ-induced diabetic mice.

Previous studies have shown that activation of caspase-3 is an initial step in muscle proteolysis.^{16,27} An increase in caspase-3-mediated cleavage of actin converts undegradable myofibrillar complex (i.e., actin/myosin complex) into substrates suitable for proteasome cleavage. In catabolic diseases,^{13,14} there is often an upregulation of the ubiquitin-proteasome proteolytic system components that results from increased gene transcription.^{8,28,29} In this study, we find that increasing muscle protein degradation is associated with caspase-3 activation and a decrease in XIAP in the muscle of insulin-deficient mice (Figure 2b). Siu and Alway³ have shown that caspase is activated and XIAP is downregulated in denervated rat skeletal muscle, which is another model for muscle atrophy. Several investigators have shown that caspase-3 activation is increased in correlation with apoptosis in models of muscle protein loss, such as chronic heart failure,^{11,12} burns injury³⁰ and disuse.^{3,31} Therefore, our results may have broad implications in other catabolic conditions associated muscle wasting, as well as with models of denervation/disuse atrophy.

XIAP is an endogenous caspase inhibitor that functions by binding to and inhibiting caspases-3, -7 and -9.^{19,20} Our data show that increasing XIAP levels by lentivirus transduction results in 80% inhibition of the muscle protein breakdown induced by insulin deficiency. As an autologous protein, XIAP offers the therapeutic advantage of minimal potential immunological complications.

There are two major pathways by which caspase-3 is activated and both are involved with muscle wasting induced by various stimuli. One is the mitochondrial pathway and the other is the death receptor pathway. In

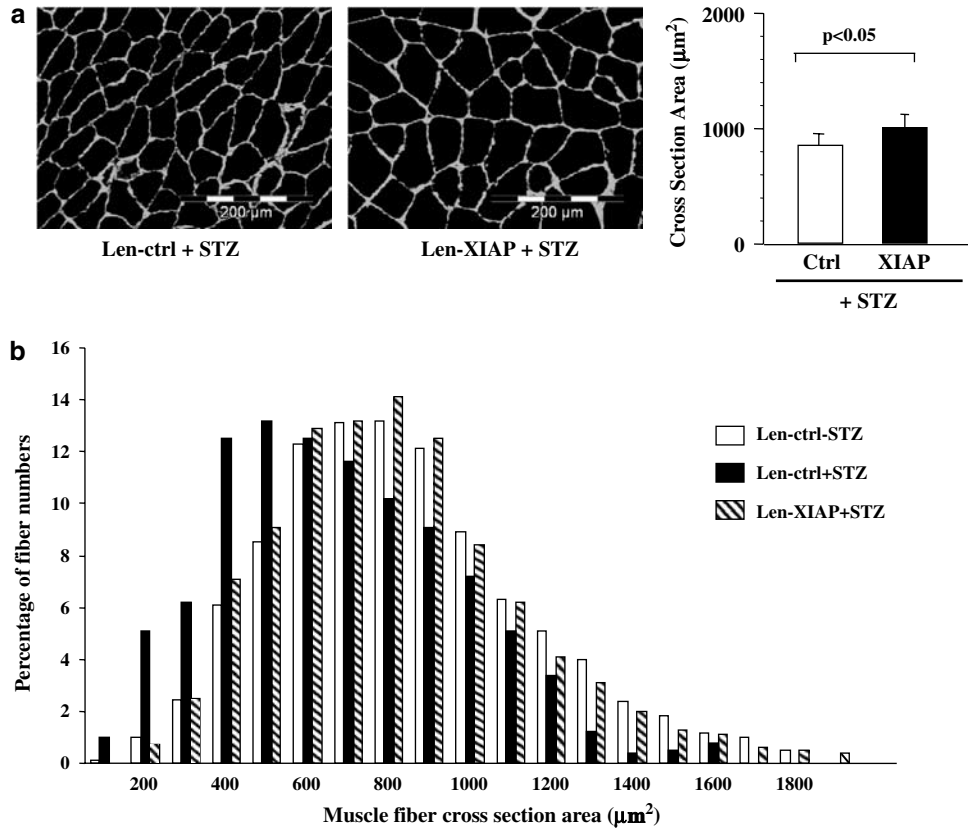


Figure 8 Effect of XIAP on muscle cross sectional area and fiber size distribution. (a) A typical cross-sectional area of plantaris muscle from STZ-treated mice without (left) or with (right) XIAP transduction. The cryosections of plantaris muscle were immunostained with anti-laminin antibody. The bar graph shows the average size of myofibers determined from six mice \times 10 sections/mouse/group with a total of 500 fibers determined. Data: mean \pm s.e., $n = 6$. (b) The frequency distribution of fiber cross-sectional area in Len-ctrl – STZ (open bar), Len-ctrl +STZ (black bar) and Len-XIAP+STZ (hatched bar) mice was calculated by the Micro-suite Five Biological Software and is presented as percent fibers/size of fibers.

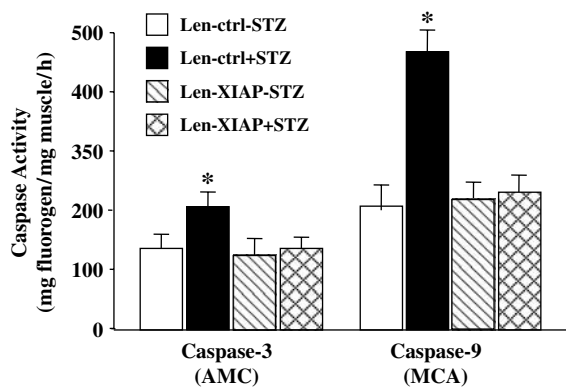


Figure 9 Effect of Len-XIAP on caspase-3 and -9 activity in insulin-deficient mice. Activation of caspase-3 and -9 in transduced muscle was measured using a fluorogenic substrate in the presence or absence of the caspase-3 or -9 inhibitors. The bars represent fluorogen released during 1 h incubation. Data: mean \pm s.e., * $P < 0.05$ vs Len-ctrl –STZ and Len-XIAP +STZ, $n = 6$.

insulin-deficient states such as the STZ-induced type I diabetes, downregulation of the phosphatidylinositol 3-kinase (PI3 K)/Akt pathway results in mitochondrial release of cytochrome *c*.¹⁶ Cytochrome *c* activates caspase-9, an initiating apoptotic protease. Activated caspase-9 then associates with APAF-1 to form an apoptosome, which activates caspase-3.^{24,27} The death

receptor pathway is triggered by the inflammatory response that increases circulating cytokines³² similar to the response seen in type II diabetes.³³ Inflammatory cytokines such as TNF α activate caspase-8 through the death receptor pathway, and caspase-8 then activates caspase-3. XIAP can inhibit the apoptotic cascade at the level of caspase 9 as well as inhibiting at the terminal step of apoptosis (caspase-3; Figure 9).¹⁸

The ATP-dependent ubiquitin–proteasome system is an important degradative pathway in the breakdown of bulk protein in muscle. Our studies provide evidence that activation of the proteasome-dependent pathway is the major contributor in muscle protein degradation in insulin-deficient animals.^{13,14} Our results demonstrate that XIAP can attenuate the proteolytic response to the proteasome-dependent proteolytic pathway in muscle of insulin-deficient diabetic mice (Figures 6b and 8). This is important because many muscle-wasting conditions share this regulatory motif (e.g., caspase-3-mediated proteasome-dependent proteolytic pathway).

Protein degradation induced by insulin deficiency was not totally blocked by increasing XIAP because the muscle fibers were not totally transduced by Len-XIAP. Studies have shown that the intracellular ratio of XIAP to caspase is critical in determining whether XIAP can successfully prevent or inhibit apoptosis. XIAP binds to caspases in either a 1:1 or 2:1 M ratio.^{20,34} We speculate that increasing transduction efficiency would improve

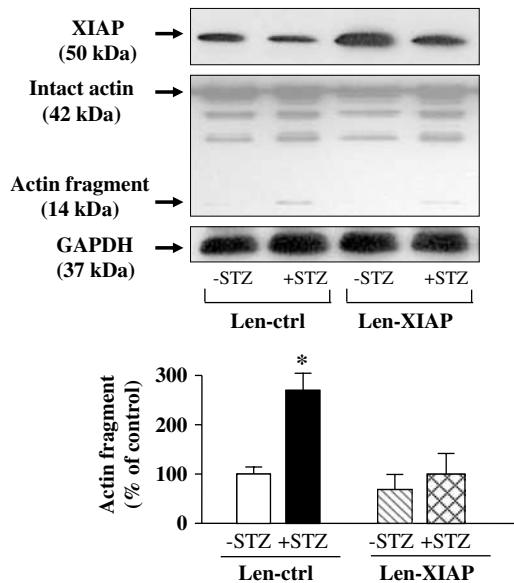


Figure 10 Effect of Len-XIAP on protein cleavage. The Western blot shows levels of XIAP (top blot), levels of the 14 kDa actin fragment and intact actin (middle blot) and the GAPDH loading control (bottom blot) in muscles harvested from STZ-treated and non-treated mice. The bar graph shows the quantity of actin cleavage calculated by the density of the 14 kDa actin fragments divided by the density of the 42 kDa intact actin and presented as percent of control values. Data: mean \pm s.e., * $P < 0.05$ vs Len-ctrl -STZ and Len-XIAP+STZ, $n = 6$.

the molar ratio and further reduce muscle protein loss in insulin-deficient states.

One advantage of lentivirus gene delivery is that a wide range of dividing and non-dividing cells *in vivo*, including post-mitotic tissue can be efficiently transduced. Although lentivirus transduction of muscle has been reported to be problematic,^{35,36} we have overcome this difficulty by adjusting the pseudotype of our lentivirus. Changing the pseudotype of lentiviruses can modify their tissue tropism.³⁷ Lentiviral vectors that are pseudotyped with vesicular stomatitis virus G glycoprotein (VSVG) can transduce a broad range of tissue and cell types and is the most common and commercially available envelope vector. However, VSVG does not work well in muscle. Kobinger *et al.*³⁸ pseudotyped the lentiviral vectors with different virus envelope glycoproteins and found that envelopes derived from the MuLV were more efficient in transducing muscle fiber.³⁷ MuLV also targets muscle satellite cells (muscle stem cells) making it a good candidate for muscle gene transfer. We pseudotyped Len-XIAP and Len-ctrl with an envelope glycoprotein from the MuLV virus, injected into newborn mice and achieved 60% transduction efficiency (Figure 4).

Studies involving adeno-associated virus reported that repeated administrations increased the gene transfer levels in skeletal muscle.³⁹ We compared the gene transfer efficiency between one, two and three injections by Len-EGFP. Although repeated transduction is unnecessary for lentivirus because lentivirus integrates into the genome of the target cells, we found that two injections elicited more efficient transduction (15% more positives vs one injection, Figure 4b), but there was no advantage to a third injection.

Another advantage of lentivirus gene delivery is that, unlike adenoviruses, lentiviruses do not transfer virus-derived coding sequence thereby sparing transduced cells from virus-specific immune responses.⁴⁰ However, therapeutic transgenes are sometimes seen as foreign antigens by the mature immune system, as XIAP is an endogenous protein, and should not cause an immune response. Because human XIAP might cause immune lesions in mice, one solution to this problem is to introduce the gene in the fetal or neonatal period, which should lead to tolerance⁴¹. We checked for immune reaction in the mice after human XIAP transduction. We injected Len-XIAP or phosphate-buffered saline (PBS) into hind-limb muscle of normal newborn mice. After 7, 21 and 42 days, hind-limb muscles were removed, sectioned and processed for histology. Analysis using light microscopy showed no pathological changes (muscle edema, lymphocyte infiltration), in the injected areas of hind-limb muscle. We saw limited central nuclei in both lentivirus and vehicle-injected gastrocnemius muscles examined 7 days after injection, which indicated an injection injury not to be a response to viral infiltration (data not shown). The central nuclei were less apparent 21 days after injection and were undetectable after 42 days. We did not find detectable anti-human XIAP antibody in the blood of mice transduced with Len-XIAP (data not shown). However, applicability to human patients will need to be addressed in future studies.

In conclusion, this is the first study to examine specifically the effect of the inhibitor of apoptosis protein, XIAP, on muscle protein catabolism induced by insulin deficiency. XIAP blunts accelerated muscle total protein degradation as well as myofibril protein breakdown in the muscles of insulin deficiency diabetic mice. XIAP blocks protein loss by inhibition of caspase-3 and reduction of the proteasome-dependent proteolytic pathway. This study also shows that lentivirus with the envelope glycoprotein from MuLV is more successful for targeting muscle fiber than other popular envelope proteins, including VSVG. Because the insulin deficiency model shares pathological characteristics (e.g., increase of caspase-3 and proteasome-dependent proteolysis) with other catabolic conditions (e.g., uremia, heart failure or denervation), our results may provide important therapeutic possibilities for treatment of muscle wasting in a number of disease states.

Materials and methods

Animals

Breeder mice (C57BLKS/J $< m+ / m+ >$) were purchased from Jackson Laboratories (Bar Harbor, ME, USA) and bred in the Department of Animal Resources at Emory University. The experiments were approved by the Institutional Animal Care and Use Committee of Emory University. Mice were housed in the animal care facility with 12-h light, 12-h dark cycle and *ad libitum* feeding until pair-feeding started. To obtain blood and tissues, mice were anesthetized with 12 mg/kg xylazine/60 mg/kg ketamine. Dissected soleus and plantaris muscles were incubated *in vitro* to measure the rates of tyrosine release. Gastrocnemius muscles were excised, flash-frozen in liquid nitrogen and stored at -80°C for descriptive experiments below.

For *in vivo* transduction using lentivirus, 10 μ l of concentrated virus (freshly prepared) were injected into hind-limb muscle over 5 min using a Hamilton syringe (30 gauge needle) within the first 24 h after birth. At 1 min after cessation of the injection, the needle was retracted an additional 1 mm and then left in place for an additional 1 min before being slowly withdrawn from the muscle. Each injection protocol took a total of 10 min. Both legs of the mouse were injected with the same type and same amount of lentivirus. A second injection of lentivirus was administered to 14-day-old mice using the same technique.

Insulin-deficient mice were produced by STZ (Pfanzstiel Lab, Waukegan IL, USA) injection using a 2-day protocol in which 150 mg/kg (prepared fresh in 0.1 M citrate buffer, pH 4.0) was given on the first day and 75 mg/kg given on the second day by intra-peritoneal injection. The control mice were injected with vehicle only. The quantity of food eaten by the STZ-treated mice was measured. Vehicle-injected control mice were paired the same amount of food.⁸

Plasma insulin was measured by the Biochemistry Core Laboratory of Emory University using the 1-2-3 ultra-sensitive mouse insulin EIA kit and mammalian insulin control set (ALPCO, Windham, NH, USA). Blood glucose concentration was measured by Accu-CHEK (Roche, Indianapolis, IN, USA).

Muscle protein degradation

Protein degradation was measured as the rate of tyrosine release from incubated muscle into the media.⁸ Individual muscles of mice were fixed at resting length on a plastic support and incubated in standard Krebs-Ringer bicarbonate (KRB) buffer (135.5 mM NaCl, 4.7 mM KCl, 24.8 mM NaHCO₃, 1 mM MgSO₄, 1 mM KH₂PO₄, 2.5 mM CaCl₂ and 10 mM glucose) containing 0.5 mM cycloheximide to block tyrosine reutilization. After a 30-min preincubation, each muscle was transferred to a flask containing fresh media and incubated at 37°C for 2 h. All incubation flasks were gassed with 95% O₂/5% CO₂ for 3 min at the beginning of the preincubation and experimental periods. Degradation of proteins was measured by assaying the free tyrosine in the trichloroacetic acid (TCA)-soluble supernatant using a fluorometric technique.⁴² The influence of insulin deficiency on different proteolytic pathways was measured by the rates of protein degradation in the muscles (soleus or plantaris) incubated with inhibitors of different pathways while the contra-lateral muscle was incubated without these inhibitors.^{8,14} Lysosomal and calcium-activated proteases were blocked by (1) adding 1 mU/ml insulin, 200 μ M valine, 170 μ M leucine, 100 μ M isoleucine and 10 mM methylamine (an inhibitor of lysosomal function); (2) deleting calcium from the KRB buffer; and (3) adding 50 μ M *trans*-epoxysuccinyl-L-leucylamido-(4-guanidinobutane) (E-64), a potent inhibitor of the calpains and the lysosomal proteases cathepsin B, D, H, and L. The ubiquitin-proteasome proteolytic pathway was inhibited by adding 20 μ M MG132 (Calbiochem Inc. San Diego, CA, USA).^{8,14}

Muscle Immunohistology

For fiber cross-sectional area, plantaris muscle were embedded under TBS Tissue Freezing Media (Fisher, Pittsburgh, PA, USA) in isopentane cooled in dry ice.

Cross sections (10 μ m) on gelatin-coated slides were fixed in 4% paraformaldehyde for 10 min. Tissue was permeabilized in 0.05% Triton X-100 (in PBS) for 10 min, and quench-fixed in 50 μ M NH₄Cl for another 10 min. Samples were blocked with 5% bovine serum albumin for 1 h, followed by incubation overnight with polyclonal anti-laminin antibody (L9393, Sigma-Aldrich; 1:50 dilution) to detect muscle membranes. Sections were further incubated for 60 min with rhodamine red-labeled anti-rabbit IgG diluted 1:100 (Jackson Immuno Research Lab, West Grove, PA, USA). Images were visualized with an Olympus 1X51 inverted fluorescence microscope and captured by SIS-CC12 CLR camera. The area of at least 500 individual myofibers per muscle was measured using the Micro-suite Five Biological Software (Olympus, Melville, NY, USA).⁴³ For a count of positive fiber numbers, we used gastrocnemius muscle that was transduced with Len-EGFP.

Production of high titer lentivirus

The cDNA coding XIAP was generated by PCR using primers; (i) 5'-aaagatccgcccacatgacttttaacagtttga-3'; (ii) 5'-aaagtcgacttaagacataaaaatttttct-3' from plasmid pEBB.XIAP,⁴⁴ and cloned into the lentivirus vector pCCL.CMV at the *Bam*H1 and *Sal*I restriction sites. The structure of the lentivirus vector (pCCL.CMV.XIAP) was verified by DNA sequencing.

HEK293H cells (Invitrogen, Carlsbad, CA, USA) were plated in 150 mm dishes with high-glucose Dulbecco's modified Eagle's medium (DMEM) containing 10% fetal bovine serum, 4 mM L-glutamine, 0.1 mM minimum essential medium (MEM) non-essential amino acids, and 1% of penicillin/streptomycin solution. Cells (80% confluence) were co-transfected with three plasmids using calcium phosphate, including 5 μ g of a packaging plasmid (pCMV Δ R8.91),^{40,45} 2 μ g of envelope plasmid (kindly provided by Drs Wilson and Kobinger),^{37,38} and 3 μ g of expression vector (a plasmid encoding human XIAP, pCCL.CMV.XIAP or pCCL.CMV.CTL for control). The serum-free DMEM without antibiotics was replaced on the second day after transfection. The conditioned medium containing the virus was collected at 48 and 72 h, filtered through 0.45- μ m cellulose acetate filter and then virus collected by low-speed centrifugation (250 g for 5 min). Virus was concentrated by centrifugation at 50 000 g for 1.5 h; viral pellets were re-suspended in a small volume (20% of the starting volume of medium) of sterile Hank's solution. Pellets from eight dishes (150-mm) were pooled and concentrated by a second ultracentrifugation for another 90 min. The final pellet was re-suspended in a very small volume (1/800 of the starting volume of medium) of sterile Hank's solution containing 4 μ g of polybrene/ml (Sigma). The virus titer was determined by serial dilution. The fresh concentrated viral preparation (10⁸ TU) was used for intramuscular injection.

Immunoblot analysis

Muscles (gastrocnemius, soleus, EDL and plantaris) were homogenized in radioimmunoprecipitation assay (RIPA) buffer. Protein concentration of the tissue lysate was determined with the Bio-Rad DC protein assay kit (Bio-Rad, Hercules, CA, USA). Proteins were subjected to Western blot analysis using previously published methods.⁴⁶ Primary antibodies used were anti-XIAP antibody

(AF822, 1:1000 dilution, R&D System Inc. Minneapolis, MN, USA), anti-glyceraldehyde 3-phosphate dehydrogenase (GAPDH) antibody (1:1000 dilution, Chemicon, Temecula, CA, USA) and anti-laminin antibody (1:100 dilution, Sigma-Aldrich, St Louis, MO, USA). Horseradish peroxidase-linked secondary antibodies were used and proteins were visualized by enhanced chemiluminescence. For determination of actin cleavage, hind-limb muscles were pulverized under liquid nitrogen and then homogenized in ice-cold hypotonic buffer. The homogenates were centrifuged (18 000 *g* for 10 min) and the resulting pellets containing the myofibrils were boiled in Laemmli sample buffer and proteins separated by 15% sodium dodecyl sulfate-polyacrylamide gel electrophoresis. Anti-actin antibody against the C-terminal actin fragment (C11 peptide, Ser-Gly-Pro-Ser-Ile-Val-His-Arg-Lys-Cys-Phe) was used to detect the 42 kDa intact actin and the 14 kDa actin fragments (1:100 dilution; Sigma-Aldrich, St Louis, MO, USA). A Bio-Rad UV-Vis Gel-doc system was used for density quantitation.

Caspase-3 and -9 activity

Gastrocnemius muscle was pulverized under liquid nitrogen and homogenized in lysis buffer (100 mM *N*-[2-hydroxyethyl] piperazine-*N*-[2-ethanesulphonic acid], 10% sucrose, 0.1% NP-40 and anti-protease cocktail 1 tablet / 10 ml (Roche 1836153), pH 7.4). The protein content of supernatants was quantified with the DC Protein Assay kit (Bio-Rad, Hercules, CA, USA). We measured the activity of caspases using a fluorogenic substrate (Ac-DEVD-7-amino-4-methylcoumarin (AMC) for caspase-3 and Ac-LEHD-MCA for caspase-9), with or without a caspase-3 inhibitor (Ac-DEVD-CHO) or caspase-9 inhibitor (Ac-LEHD-CHO) (Promega, Madison, WI, USA) in the caspase assay buffer provided with the CaspACE Assay System (Promega, Madison, WI, USA). The incubation temperature for fluorogen (AMC) release is 37°C for caspase-3 and 4°C methylcoumarylamide (MCA) for caspase-9 for 1 h. Fluorescence was measured in a fluorometer (Shimadzu) with a 380 nm excitation wavelength and a 460 nm emission wavelength. The difference between the substrate cleavage activity levels in the presence and absence of caspase inhibitor was used to calculate the contribution of caspase-3 and -9 activities.

Proteasome activity

To measure proteasome proteolytic activity,⁴³ hind-limb muscles were pulverized under liquid nitrogen and homogenized in lysis buffer (Tris-HCl, pH 7.4, 50 mM, MgCl₂ 5 mM, sucrose 250 mM, and freshly added dithiothreitol 2 mM and ATP 2 mM). Lysates were pelleted by centrifugation (5 min, 400 *g*). The supernatant from the centrifugation was clarified by two additional centrifugations: 1 h at 100 000 *g* for the 26S proteasome, then 5 h at 100 000 *g* to obtain the 20S proteasome.¹⁵ Pellets were re-suspended in assay buffer (Tris-HCl, pH 7.4, 50 mM, MgCl₂ 5 mM, ATP 2 mM and glycerol 20%) to measure the proteasome proteolytic activity. Chymotrypsin-like activity was determined from the release of AMC from the fluorogenic peptide substrate LLVY-AMC (*N*-Suc-Leu-Leu-Val-Tyr-AMC) using the Proteasome Activity Assay Kit (Chemicon Int., Temecula, CA, USA). Lactacystin, a specific inhibitor of the proteasome,

(200 μM, Calbiochem, San Diego, CA, USA), was included with some samples to identify specific proteasomal proteolytic activity. Fluorescence was measured in a fluorometer (Shimadzu) using an excitation and emission wavelengths of 380 and 460 nm, respectively.

Statistical analysis

Data were expressed as the mean ± s.e. densitometric data for blots were expressed as a percentage of the mean density of control after normalization to loading controls. To identify significant differences between two groups, comparisons were made by using the Student's *t*-test. Differences with *P*-values < 0.05 were considered significant.

Abbreviations

EDL, extensor digitorum longus; MuLV, murine leukemia virus; STZ, streptozotocin; XIAP, X-chromosome linked inhibitor of apoptosis protein.

Acknowledgements

We thank Dr Didier Trono for providing the packaging plasmid; Drs James Wilson and Gary Koringer for providing the five lentivirus envelope plasmids; Dr Yili Yang for the pEBB.XIAP plasmid, Dr Joe M LeDoux for pCCL.CMV.GFP plasmid. We thank Dr Russ Price and Dr James Bailey for their critical reading of this manuscript. This study was supported by a Norman S Coplion Extramural Research Grant from Satellite Health, an American Diabetes Association Junior Faculty Award 1-04-JF-48 and NIH R21 Grant DK62796 to XHW, and NIH R01 DK062081 to JDK.

References

- 1 Griffiths RD. Muscle mass, survival, and the elderly ICU patient. *Nutrition* 1996; **12**: 456–458.
- 2 Windsor JA, Hill GL. Risk factors for postoperative pneumonia. The importance of protein depletion. *Ann Surg* 1988; **208**: 209–214.
- 3 Siu PM, Alway SE. Mitochondria-associated apoptotic signalling in denervated rat skeletal muscle. *J Physiol* 2005; **565**: 309–323.
- 4 Leeuwenburgh C, Gurley CM, Strotman BA, Dupont-Versteegden EE. Age-related differences in apoptosis with disuse atrophy in soleus muscle. *Am J Physiol Regul Integr Comp Physiol* 2005; **288**: R1288–R1296.
- 5 Siu PM, Pistilli EE, Butler DC, Alway SE. Aging influences cellular and molecular responses of apoptosis to skeletal muscle unloading. *Am J Physiol Cell Physiol* 2005; **288**: C338–349.
- 6 Galban VD, Evangelista EA, Migliorini RH, do Carmo Kettelhut I. Role of ubiquitin-proteasome-dependent proteolytic process in degradation of muscle protein from diabetic rabbits. *Mol Cell Biochem* 2001; **225**: 35–41.
- 7 Nair KS, Ford GC, Ekberg K, Fernqvist-Forbes E, Wahren J. Protein dynamics in whole body and in splanchnic and leg tissues in type I diabetic patients. *J Clin Invest* 1995; **95**: 2926–2937.
- 8 Bailey JL, Wang X, England BK, Price SR, Mitch WE. The acidosis of chronic renal failure activates muscle proteolysis in rats by augmenting transcription of genes encoding proteins of the ATP-dependent ubiquitin-proteasome pathway. *J Clin Invest* 1996; **97**: 1447–1453.

- 9 Mansoor O, Beaufriere B, Boirie Y, Ralliere C, Taillandier D, Aourousseau E *et al*. Increased mRNA levels for components of the lysosomal, Ca²⁺-activated, and ATP-ubiquitin-dependent proteolytic pathways in skeletal muscle from head trauma patients. *Proc Natl Acad Sci USA* 1996; **93**: 2714–2718.
- 10 Fang CH, Tiao G, James H, Ogle C, Fischer JE, Hasselgren PO. Burn injury stimulates multiple proteolytic pathways in skeletal muscle, including the ubiquitin-energy-dependent pathway. *J Am Coll Surg* 1995; **180**: 161–170.
- 11 Vescovo G, Volterrani M, Zennaro R, Sandri M, Ceconi C, Lorusso R *et al*. Apoptosis in the skeletal muscle of patients with heart failure: investigation of clinical and biochemical changes. *Heart* 2000; **84**: 431–437.
- 12 Libera LD, Zennaro R, Sandri M, Ambrosio GB, Vescovo G. Apoptosis and atrophy in rat slow skeletal muscles in chronic heart failure. *Am J Physiol* 1999; **277**: C982–C986.
- 13 Price SR, Bailey JL, Wang X, Jurkovitz C, England BK, Ding X *et al*. Muscle wasting in insulinopenic rats results from activation of the ATP-dependent, ubiquitin–proteasome proteolytic pathway by a mechanism including gene transcription. *J Clin Invest* 1996; **98**: 1703–1708.
- 14 Mitch WE, Bailey JL, Wang X, Jurkovitz C, Newby D, Price SR. Evaluation of signals activating ubiquitin–proteasome proteolysis in a model of muscle wasting. *Am J Physiol* 1999; **276**: C1132–1138.
- 15 Solomon V, Goldberg AL. Importance of the ATP-ubiquitin–proteasome pathway in the degradation of soluble and myofibrillar proteins in rabbit muscle extracts. *J Biol Chem* 1996; **271**: 26690–26697.
- 16 Du J, Wang X, Mierles C, Bailey JL, Debigare R, Zheng B *et al*. Activation of caspase-3 is an initial step triggering accelerated muscle proteolysis in catabolic conditions. *J Clin Invest* 2004; **113**: 115–123.
- 17 Deveraux QL, Reed JC. IAP family proteins – suppressors of apoptosis. *Genes Dev* 1999; **13**: 239–252.
- 18 Holcik M, Korneluk RG. XIAP, the guardian angel. *Nat Rev Mol Cell Biol* 2001; **2**: 550–556.
- 19 Deveraux QL, Roy N, Stennicke HR, Van Arsdale T, Zhou Q, Srinivasula SM *et al*. IAPs block apoptotic events induced by caspase-8 and cytochrome c by direct inhibition of distinct caspases. *EMBO J* 1998; **17**: 2215–2223.
- 20 Deveraux QL, Takahashi R, Salvesen GS, Reed JC. X-linked IAP is a direct inhibitor of cell-death proteases. *Nature* 1997; **388**: 300–304.
- 21 Xu D, Bureau Y, McIntyre DC, Nicholson DW, Liston P, Zhu Y *et al*. Attenuation of ischemia-induced cellular and behavioral deficits by X chromosome-linked inhibitor of apoptosis protein overexpression in the rat hippocampus. *J Neurosci* 1999; **19**: 5026–5033.
- 22 Case SS, Price MA, Jordan CT, Yu XJ, Wang L, Bauer G *et al*. Stable transduction of quiescent CD34(+)/CD38(–) human hematopoietic cells by HIV-1-based lentiviral vectors. *Proc Natl Acad Sci USA* 1999; **96**: 2988–2993.
- 23 Kugler S, Straten G, Kreppel F, Isenmann S, Liston P, Bahr M. The X-linked inhibitor of apoptosis (XIAP) prevents cell death in axotomized CNS neurons *in vivo*. *Cell Death Differ* 2000; **7**: 815–824.
- 24 Liu X, Kim CN, Yang J, Jemmerson R, Wang X. Induction of apoptotic program in cell-free extracts: requirement for dATP and cytochrome c. *Cell* 1996; **86**: 147–157.
- 25 Larochele A, Peng KW, Russell SJ. Lentiviral vector targeting. *Curr Top Microbiol Immunol* 2002; **261**: 143–163.
- 26 Hunter RB, Kandarian SC. Disruption of either the Nfkb1 or the Bcl3 gene inhibits skeletal muscle atrophy. *J Clin Invest* 2004; **114**: 1504–1511.
- 27 Lee SW, Dai G, Hu Z, Wang X, Du J, Mitch WE. Regulation of muscle protein degradation: coordinated control of apoptotic and ubiquitin–proteasome systems by phosphatidylinositol 3 kinase. *J Am Soc Nephrol* 2004; **15**: 1537–1545.
- 28 Marinovic AC, Zheng B, Mitch WE, Price SR. Ubiquitin (UbC) expression in muscle cells is increased by glucocorticoids through a mechanism involving Sp1 and MEK1. *J Biol Chem* 2002; **277**: 16673–16681.
- 29 Du J, Mitch WE, Wang X, Price SR. Glucocorticoids induce proteasome C3 subunit expression in L6 muscle cells by opposing the suppression of its transcription by NF-kappa B. *J Biol Chem* 2000; **275**: 19661–19666.
- 30 Yasuhara S, Perez ME, Kanakubo E, Yasuhara Y, Shin YS, Kaneki M *et al*. Skeletal muscle apoptosis after burns is associated with activation of proapoptotic signals. *Am J Physiol Endocrinol Metab* 2000; **279**: E1114–1121.
- 31 Allen DL, Linderman JK, Roy RR, Bigbee AJ, Grindeland RE, Mukku V *et al*. Apoptosis: a mechanism contributing to remodeling of skeletal muscle in response to hindlimb unweighting. *Am J Physiol* 1997; **273**: C579–C587.
- 32 Deveraux QL, Leo E, Stennicke HR, Welsh K, Salvesen GS, Reed JC *et al*. Cleavage of human inhibitor of apoptosis protein XIAP results in fragments with distinct specificities for caspases. *EMBO J* 1999; **18**: 5242–5251.
- 33 Wang XL, Zhang L, Youker K, Zhang MX, Wang J, Lemaire SA *et al*. Free fatty acids inhibit insulin signaling-stimulated endothelial nitric oxide synthase activation through upregulating PTEN or inhibiting Akt kinase. *Diabetes* 2006; **55**: 2301–2310.
- 34 Roy N, Mahadevan MS, McLean M, Shuttler G, Yaraghi Z, Farahani R *et al*. The gene for neuronal apoptosis inhibitory protein is partially deleted in individuals with spinal muscular atrophy. *Cell* 1995; **80**: 167–178.
- 35 Trono D. HIV-based vectors: getting the best out of the worst. *J Gene Med* 2000; **2**: 61–63.
- 36 Trono D. Lentiviral vectors: turning a deadly foe into a therapeutic agent. *Gene Therapy* 2000; **7**: 20–23.
- 37 MacKenzie TC, Kobinger GP, Kootstra NA, Radu A, Sena-Esteves M, Bouchard S *et al*. Efficient transduction of liver and muscle after in utero injection of lentiviral vectors with different pseudotypes. *Mol Therapy* 2002; **6**: 349–358.
- 38 Kobinger GP, Louboutin JP, Barton ER, Sweeney HL, Wilson JM. Correction of the dystrophic phenotype by *in vivo* targeting of muscle progenitor cells. *Hum Gene Therapy* 2003; **14**: 1441–1449.
- 39 Riviere C, Danos O, Douar AM. Long-term expression and repeated administration of AAV type 1, 2 and 5 vectors in skeletal muscle of immunocompetent adult mice. *Gene Therapy* 2006; **13**: 1300–1308.
- 40 Zufferey R, Nagy D, Mandel RJ, Naldini L, Trono D. Multiply attenuated lentiviral vector achieves efficient gene delivery *in vivo*. *Nat Biotechnol* 1997; **15**: 871–875.
- 41 Seppen J, van Til NP, van der Rijt R, Hiralal JK, Kunne C, Elferink RP. Immune response to lentiviral bilirubin UDP-glucuronosyltransferase gene transfer in fetal and neonatal rats. *Gene Therapy* 2006; **13**: 672–677.
- 42 Clark AS, Mitch WE. Comparison of protein synthesis and degradation in incubated and perfused muscle. *Biochem J* 1983; **212**: 649–653.
- 43 Wang X, Hu Z, Hu J, Du J, Mitch WE. Insulin resistance accelerates muscle protein degradation: activation of the ubiquitin–proteasome pathway by defects in muscle cell signaling. *Endocrinology* 2006; **147**: 4160–4168.
- 44 Yang Y, Fang S, Jensen JP, Weissman AM, Ashwell JD. Ubiquitin protein ligase activity of IAPs and their degradation in proteasomes in response to apoptotic stimuli. *Science* 2000; **288**: 874–877.
- 45 Dull T, Zufferey R, Kelly M, Mandel RJ, Nguyen M, Trono D *et al*. A third-generation lentiviral vector with a conditional packaging system. *J Virol* 1998; **72**: 8463–8471.
- 46 Kim D, Sands JM, Klein JD. Changes in renal medullary transport proteins during uncontrolled diabetes mellitus in rats. *Am J Physiol Renal Physiol* 2003; **285**: F303–F309.